

SCINTILLATOR BARREL DETECTOR OF THE ALICE EXPERIMENT

V. Kolosov, Yu. Kharlov, G. Khaustov, A. Levin, Yu. Orlov,
S. Polovnikov, V. Polyakov, S. Sadovsky, V. Samoylenko,
A. Semenov, A. Shtannikov, A. Surkov

Institute for High Energy Physics, Protvino, Russia.

Abstract

The Scintillator Barrel (ScB) is the first level trigger detector whose task is to cover the central region of the ALICE setup. The physical goals of the ScB, its construction, electronics and trigger performance as well as results of the ScB prototype tests are described in detail.

1 Introduction

ALICE [1] should operate with different ion species including pp collisions. Both the collision luminosity and the particle density in the final state, vary by 3 orders of magnitude in different collisions, *i.e.* from $dN/dy = 7.2$ in the case of pp collisions up to 8000 in the central PbPb collisions. Therefore the requirements to trigger detectors in these cases are essentially different.

The two main trigger detectors of the ALICE, the ZDC and FMD, are specially designed and well suited to trigger for minimum bias or central events in heavy-ion collisions. However, in pp reactions a certain bias at low multiplicity might occur because the ZDC can not be used and the FMD does not cover the acceptance of ALICE in the central region.

The scintillator barrel, whose task is to cover the central region of the ALICE setup, is the special first level trigger detector which can be used for:

- central trigger in ion collision.
- low multiplicity trigger in pp-collisions.
- cosmic trigger for the ALICE setup testing and calibration.
- low multiplicity trigger in ion collision, which can be used together with the ZDC for selection of two photon processes with only charged particles in the final state, details see elsewhere [2].

The ScB, being reasonably priced, can essentially increase the trigger potential of ALICE.

2 Construction and readout

In pseudorapidity the ScB should cover the central region $|\eta| < 0.9$, where the main detectors of the ALICE will be installed. The length of the ScB along the beam axis is equal to 5.6 m. Its inner radius is 2.75 m, and the outer radius is 2.95 m. It will be placed between TPC and PID system.

The general view of the scintillator barrel is presented in fig.1. It consists of 24 supermodules. The granularity of the ScB is mainly defined by requirements of the trigger quality. Each supermodule ($1.5 \times 2.75 \text{ m}^2$, fig.2) includes two layers of overlapping scintillator tiles (140 tiles in one supermodule, 3360 tiles in the full barrel). The tile sizes in outer and inner layers are $0.6 \times 17 \times 18.5 \text{ cm}^3$ and $0.6 \times 34 \times 37 \text{ cm}^3$ respectively. Each four tiles in the outer layer of the supermodule overlap with one tile of the inner layer. The tiles in the supermodules are supported by honeycomb structure. The transverse radiation length of the barrel is $\sim 3\%$ of X_0 .

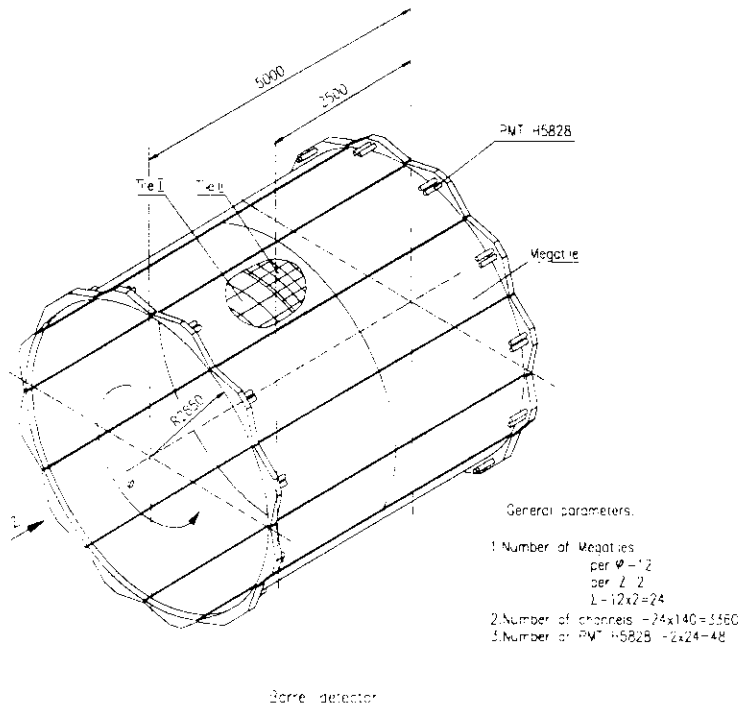


Figure 1: The general view of the scintillator barrel.

The method of scintillation light collection by WLS fibers developed in [3, 4] is used. The light from a tile is collected by four WLS fibers placed in "sigma" shape grooves in the scintillator (fig. 2). The fiber edge inside the scintillator is polished and thin aluminium layer is evaporated on it as a mirror to provide 80~90% reflection efficiency. Outside the scintillator WLS fibers are connected to clear fibers via optical connectors. The clear fibers transport light to the multianode photomultiplier. Light loss in the optical connector doesn't exceed 10%.

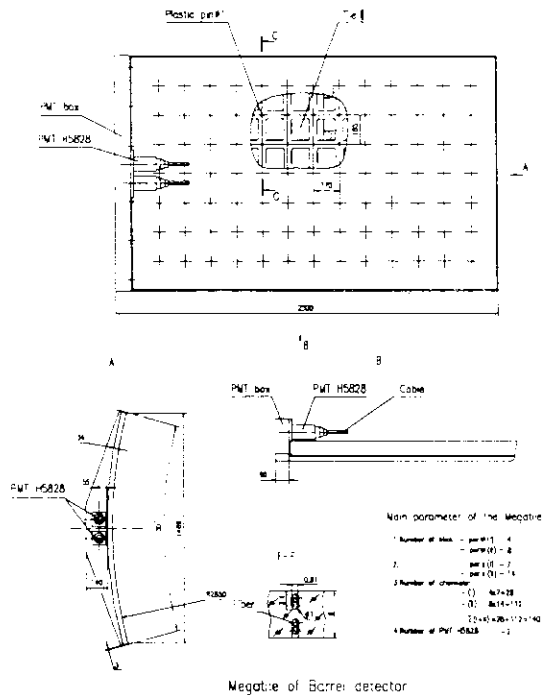


Figure 2: The supermodule of the scintillator barrel.

The length of the clear fibers depends on the tile position in the barrel. It can be chosen to provide simultaneous arrival of the light signals to the photomultiplier. For the case of PbPb collisions the difference in time of flight for charged particles were simulated using the HIJING program for pseudorapidity $\eta = 0$ and $|\eta| = 1$, see fig. 3. The maximum time difference is equal to ~ 4 ns. Therefore ~ 1 meter of fiber is enough to compensate it, but this leads to a 15÷20% losses in the light yield.

Light attenuation length of the clear fibers is more than 5 meters. For tiles placed in the centre of the barrel the length of fibers is about 4 m and maximum light loss does not exceed 60 %.

Multianode photomultipliers, also called position-sensitive PMT, are now under study to be used in scintillating fiber technology, precise scintillator hodoscopes, vertex detectors etc. Recently RD-17 project [5] at CERN (FAROS collaboration) has obtained excellent results with the new Hamamatsu H5828 multianode PMT and scintillating fiber hodoscope. This photomultiplier demonstrates low single electron noise (less than 10^4 e^{-1}), good quantum efficiency for blue light, high gain and low crosstalk (less than 2%) [6].

In the ScB we suppose to use the similar technique. Two 80 anodes Hamamatsu H5828 photomultipliers, which can operate in magnetic field parallel to the PMT axis, are enough for the barrel supermodule (140 tiles). In each PMT 70 channels are used for signal readout, 4 channels are used for precise positioning of the bundle with respect to the PMT and 6 channels are reserved.

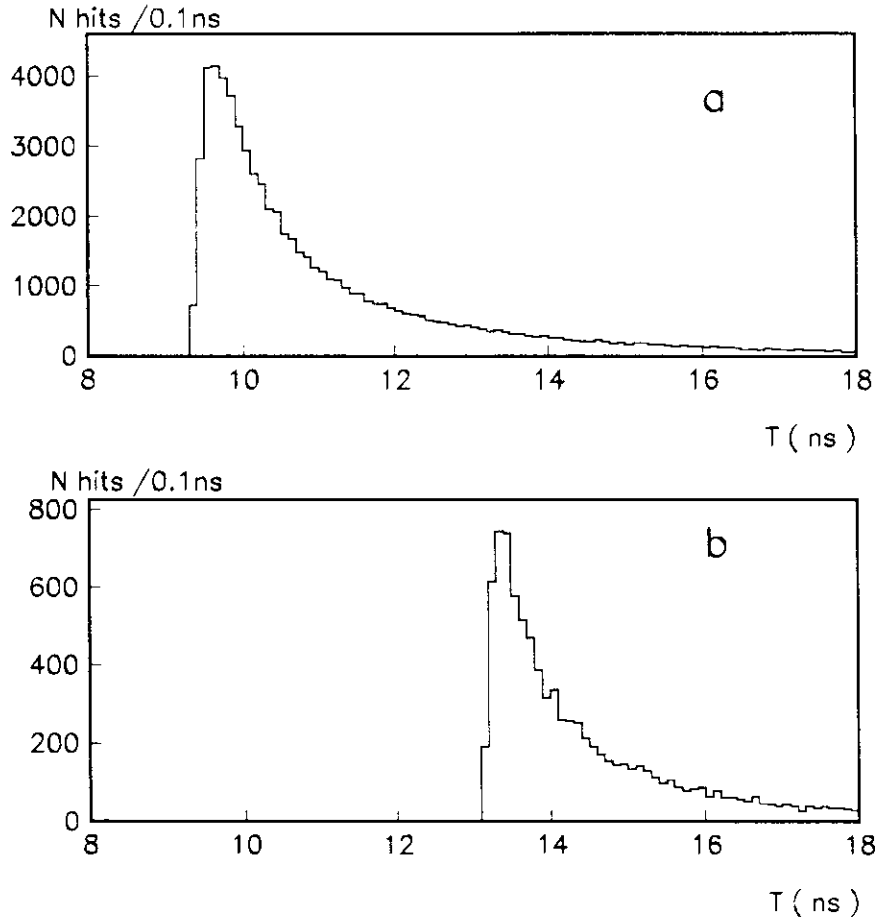


Figure 3: The time of flight distributions for charge particles crossing ScB tiles for pseudorapidity $\eta = 0$ (a) and $|\eta| = 1$ (b) for case of Pb-Pb collisions simulated by HIJING code.

The fiber bundle with additional fiber for PMT gain monitoring is fixed on movable support providing positioning of the bundle with precision better than 0.1 mm in X and Y directions by micrometric screws. For the monitoring of the bundle centering at the assembly stage, the signals from four auxiliary fibers placed in the corners of the fiber matrix are used.

3 Test results

Two types of scintillator tiles, T1 ($10 \times 10 \times 1 \text{ cm}^3$) and T2 ($15 \times 15 \times 1 \text{ cm}^3$) with different WLS fibers (round and square cross sections) have been tested with ^{106}Ru radioactive source as well as in hadron beam of the PS accelerator in CERN. The circular grooves

with width 1.1 mm and depth 3 mm and diameters of 9.5 cm and 14.5 cm for T1 and T2 respectively, were machined in the scintillator tiles.

The polystyrene scintillator with 1.5% PTP (para-terphenyl) + 0.01% POPOP (1,4-bis-[2-(5-phenyloxazolyl)]-benzene) dopants and polystyrene multiclading WLS fibers with K-27 dopant, produced in Russia, were used.

Two 70 cm length fibers and PMT FEU-84 (quantum efficiency $\sim 8\%$ for green light 500-550 nm) were used for signal readout of T1. The number of photoelectrons produced by the minimum ionizing particle (MIP) in T1 was measured to be 14 ph.e. (fig. 4). Thus, after 4 meters of clear fiber we expect to have about 6 ph.e.

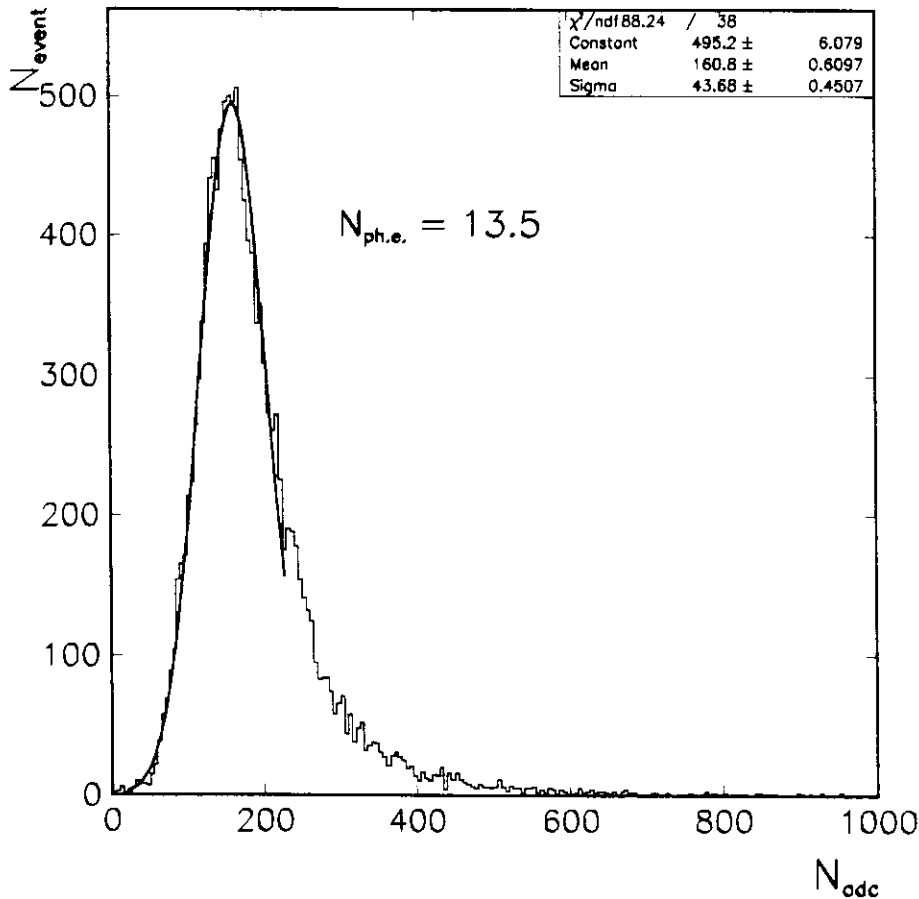


Figure 4: The amplitude spectrum for minimum ionizing particle crossing scintillator tile.

Six samples of T2 tile have been tested. These T2 tiles were read out by PMT FEU-84 and four 1.5 m long WLS fibers, of which about 50 cm were placed into grooves and the rest 1 m was used for light transportation. The light attenuation in such fibers is equivalent to that in 4 m clear fibers. The number of photoelectrons

per MIP for T2 tiles is equal to 12 ph.e. and has small spread (less than 20%). It is enough for almost one hundred percent detection efficiency of a single charged particle.

A study of the tiles with the Hamamatsu H5828 multianode PMT was performed together with the FAROS collaboration team. The number of photoelectrons per MIP passing T2 tile was measured to be 4 ph.e. The difference between the last number and the results obtained with FEU-84 PMT can be completely explained by the low quantum sensitivity of the Hamamatsu H5828 to green light: this type of PMT was optimized for scintillation light detection. Thus it is necessary to optimize photocathode of the multianode PMT to green light to get similar results as obtained with FEU-84. Another possibility to improve the light yield is to provide good optical contact in scintillator-fiber gap i.e. to glue WLS fiber to the scintillator. This could increase the light yield by a factor of $1.5 \div 2.0$.

Measurements of T2 tiles with square WLS fibers ($1 \times 1 \text{ mm}^2$ cross section) demonstrate 30% better light yield as compared to the round fibers (1 mm diameter). A nonuniformity of response along the surface of the tiles for both T1 and T2 measured with ^{106}Ru source does not exceed $\pm 10\%$.

4 Electronics

The physical performance of the ScB depends strongly on the front-end and trigger electronics which will be used. The block-scheme of the electronics shown in fig. 5 is proposed to fit the requirements of the multi-option trigger. The PMT signals from an inner tile and one of the four outer tiles after amplifier-discriminator coincide to form one-bit information for the shift register. The amplifier-discriminator has an additional analog output which provide the delayed and calibrated signal for the amplitude analysis and analog summing. The calibration of the ScB can be performed at the stage of the setup selftesting with cosmic trigger, see below. The gate for ADC and strobe for the registers is formed by fast OR of entire barrel (or upper half of the barrel in the case of cosmic trigger). To count hits in each supermodule the high frequency counters are used. The final number of hits in the barrel is calculated by the fast ALU. To read out the hit positions the information from the shift registers can be loaded in latches before the start of the shifting.

The trigger electronics of the ScB can operate in two different modes: the bit summing with subsequent discrimination on the hit amount and the Analog Summing (AS) of signals from the tiles in the outer layer. The first one will be useful in the case of low multiplicity pp and CaCa collisions as well as in PbPb collisions to suppress the peripheral interactions of the ions. The second one allows an impact parameter measurement in PbPb collisions, when the hit saturation in the ScB occurs.

If fast ECL chips (MECL III for exm.) will be used, the expected value of trigger decision time is about $1 \mu\text{s}$ in the case of bit summing. This is sufficient for trigger requirements in pp collisions. The analog summing of the signals can be performed during 100 – 200 ns, that may be useful also for the case of CaCa collisions, where the event rates can be increased up to 10^7 events/s .

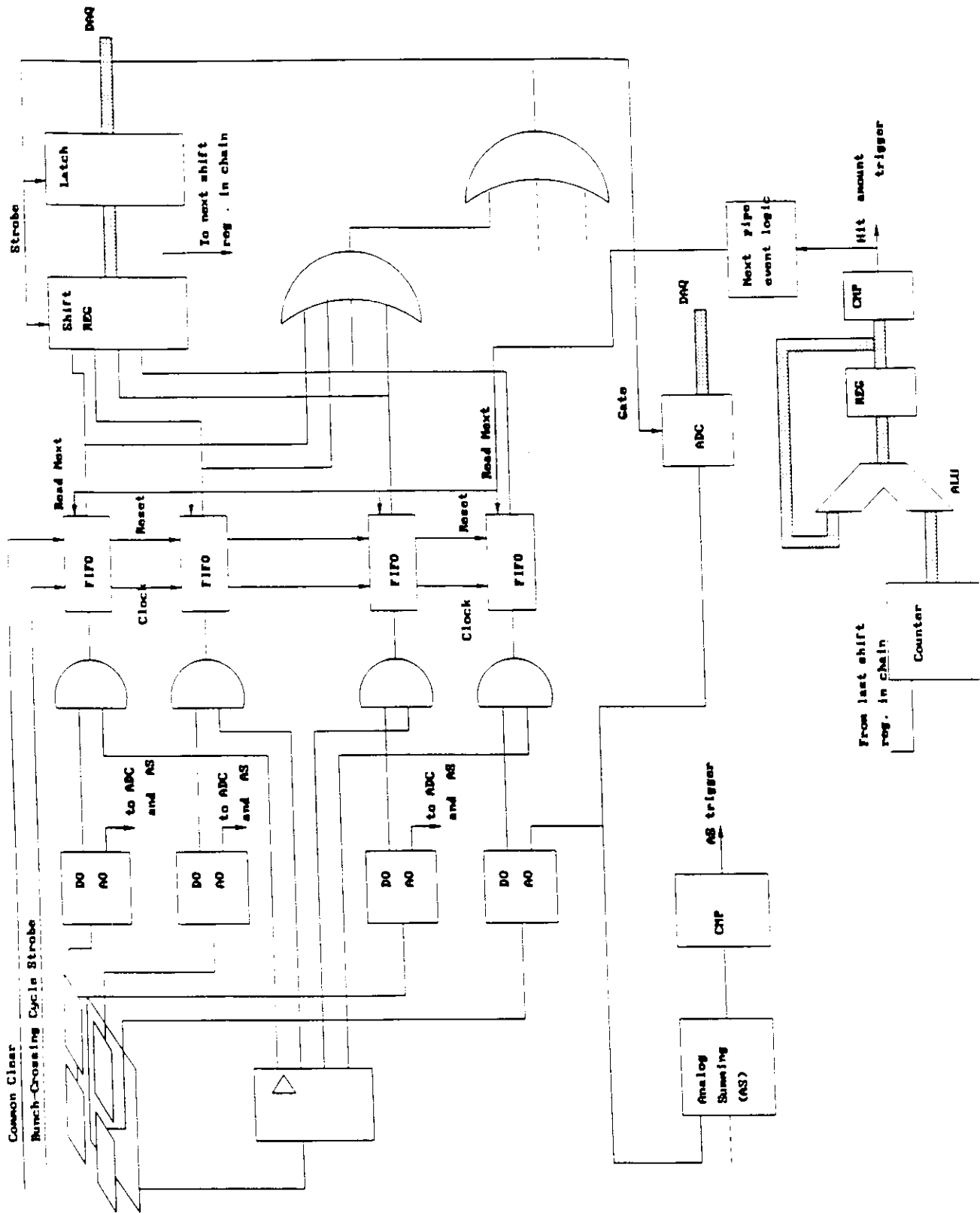


Figure 5: The block scheme of the electronics for the SeB.

In order to improve the efficiency of the bit summing trigger the "pipe" scheme based on the "First-In-First-Out" memory is suggested, see fig.5. The bunch-crossing strobe can be used as clock signal for FIFO memory. Thus we have hit information in each bunch crossing i.e. every 25 ns. The depth of the pipe is defined by expected event rate. With one event per 5 bunches 8-bit FIFO should be enough. During the decision time of trigger the FIFO is filled with coming bunches and blocked when it will be full. If the trigger decision is "NO", the next event from FIFO is selected and so on. When the needed event is found, the trigger sends its number to the second level trigger. The event number synchronization can be achieved by the "Common Clear" signal which resets the FIFO and the counter.

5 Neural Net trigger

Another variant of the trigger electronics for ScB can be realized by means of the Feed-Forward Neural Net (FFNN), based on manufactory produced NN chips. In this case the analog outputs of the amplifier-discriminators (see fig. 5) can be used directly as the sources of the input signals for analog NN.

The most widely used NN chip in high energy physics is ETANN 80170NX [7, 8] of INTEL. This chip has internal architecture 64 - 64 - 64 or 128 - 64 neurons. The time propagation for one layer is $\simeq 1 \mu s$. Recently the new very fast NeuroClassifier [9] chip was announced. This chip has 70 input neurons at bandwidth 4 *GByte/s*, 6 hidden layers and one output neuron. It has propagation time only 20 *ns*. The precision of the analog multiplication/addition operation is quite enough (5 bits). It is significant that the decision time is independent on the input pattern, because there are no internal loops in the chip for pattern processing.

Looking ahead the NN chip like the NeuroClassifier can be used in NN for ScB trigger. One NN chip processes one multianode PMT (two NN chips for each barrel supermodule having 140 channels). The result of supermodule processing can be obtained after 100 - 200 ns. The NN training procedure based on moderate learning methods decreases the output net error to the level less than 10^{-2} .

In parallel with trigger processing the NN can be used for determination of the particle multiplicities in the ScB supermodules, energy estimation in each supermodule as well as for identification of events with given topology, including jet topology.

The NN hardware can solve also such problems as on-line testing and calibration of the ScB. By loading a special weight matrix it is possible to switch on/off each channel of the ScB for checking and calibration. The adjustment of channel gain is performed by changing of weight coefficient of the matrix, thus we have also a soft-driving amplifier for each channel.

One should expect fast development of the speed and complexity of the NN hardware along with a dramatically cost decreasing. We believe that in the near future the price of NN chips will be around 100 \$. For this reason it possible to create the fast NN trigger system for ScB with outstanding price/performance ratio.

6 Trigger and physics performance

In the case of PbPb collisions the interaction rate is 8000 events/s at luminosity of $10^{27} \text{ cm}^{-2}\text{s}^{-1}$. The aim of the first level trigger is to suppress peripheral collisions with impact parameter $b > 8 \text{ fm}$. The multiplicities of charged particles hitting the ScB at different values of the impact parameter b were estimated using the HIJING program, as shown in fig. 6a. At $b \approx 9 \text{ fm}$ on average 2500 charged particles hit the ScB. Therefore to identify the events with such and smaller multiplicities (and therefore with 9 fm and higher values of the impact parameter) the barrel should contain about 2500 effective tiles. At the chosen granularity of the ScB ($N_{\text{tile}}^{\text{outer}} = 2688$) the barrel saturation is expected at $b \leq 8 \text{ fm}$, as shown in fig.6b. The trigger requirement on the number of firing tiles, $N_{\text{fire}} > 2500$ leads to the effective suppression of the peripheral PbPb-collisions, selecting about 10% of the events.

Note that impact parameter measurements for selected events will be impossible on the basis of hit counting owing to saturation of the barrel at $b < 8 \text{ fm}$. Nevertheless the impact parameter could be measured using analogue summation of the signal amplitudes, or could be reconstructed off-line if the amplitudes are measured and recorded for all firing tiles. The on-line procedures will be more precise if prior tile calibration will be performed on cosmic events, as discussed below. Both options require equalization of delay time of signals from different tiles. The accuracy of the total particle number measurement is defined by precision of the calibration procedure and uniformity of tile response. Starting from a number of charged particle 1000 we can expect 1% statistical accuracy in particle number measurements.

In the case of CaCa collisions the charged particle multiplicity is 7 times smaller than in PbPb collisions, and therefore the ScB will allow the measurement of the impact parameter in the full b-range, $b \leq 10 \text{ fm}$, on the bases of firing tile counting.

The expected CaCa luminosity (up to $5 \cdot 10^{30} \text{ cm}^{-2}\text{s}^{-1}$) leads to the interaction rate of the ions higher than 10^7 s^{-1} . Thus with $\sim 10\%$ probability the CaCa interactions can occur in the neighboring bunch crossing separated by 25 ns in time. This essentially increases the requirements to the pulse timing from different tiles of the barrel. The compensation of the systematic delay of signals from different tiles (up to 4 ns , fig.3) can be quite useful in this case as well as the 'pipe' scheme of the trigger electronics discussed above.

In the case of pp collisions the interaction rate is 10^5 s^{-1} but the particle density is very low: $dN_{\text{charge}}/dy = 7.2$. The ScB can be used effectively to select low multiplicity events, *i.e.* those with two or more charged particles in the barrel. The probability of one tile firing randomly P_{fire} during the time gate τ is equal to

$$P_{\text{fire}} = \tau f_{\text{noise}}, \quad (1)$$

where f_{noise} is the noise frequency in the PMT channel. The probability of a single random hit in the ScB (the coincidence of the signal from an inner layer tile with one of the four outer tiles) is equal to

$$P_{\text{hit}} = 4P_{\text{fire}}^2. \quad (2)$$

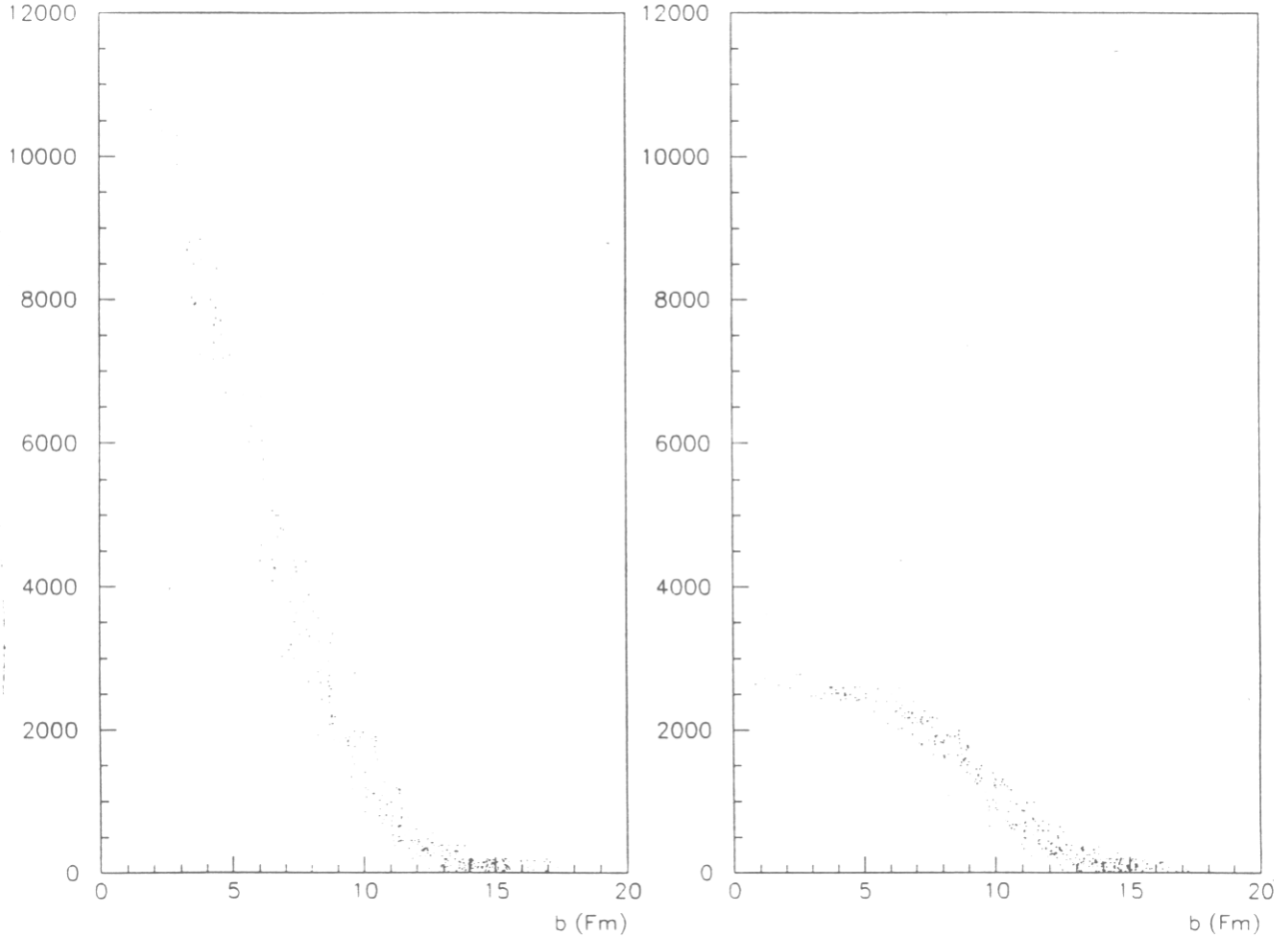


Figure 6: **a)** The particle multiplicity in the scintillator barrel and **b)** the active tail multiplicity in the scintillator barrel as function of the impact parameter for PbPb collisions.

The average number of random hits is then

$$\langle n_{fire} \rangle = N_{tiles}^{outer} P_{fire}, \quad (3)$$

where N_{tiles}^{outer} is the outer tail number ($N_{tiles}^{outer} = N_{tiles}^{tot}/1.25$), and therefore the probability of k -hits in the barrel is

$$P_{fire}(k) = \frac{1}{k!} \langle n_{fire} \rangle^k e^{-\langle n_{fire} \rangle}. \quad (4)$$

Taking $f_{noise} = 10^4 Hz$ and $\tau = 20$ ns we obtain for the probability of 2 random hits during the time gate the expression

$$P_{hit}(2) \approx 5 \times 10^{-9}. \quad (5)$$

The last value should be compared with the pp-event probability during the same time:

$$P_{pp} = L_{pp} \sigma_{pp}^{inel} \tau = 2 \cdot 10^{-4} \quad (6)$$

at $L_{pp} = 10^{30} \text{ cm}^{-2} \text{ s}^{-1}$. Thus the rate for 2 and more random hits is negligible compared with the inelastic pp-event rate.

The other application of the ScB in the case of pp-collisions is to select the particles from TPC, which belong to the same event. Really, during the deadtime of the TPC (200 μs) 20 pp-interactions will occur and therefore about 260 charged particles will pass through the TPC and will be detected as one event (pile up). But for all particles hit the ScB the time mark exist (hits distribution in the ScB for each event), which allows to select from TPC the particles hitted the barrel in different events. The only small energetic particles which will not achieve the ScB due to rotation in the magnetic field can not be identified.

7 Cosmic trigger

The ScB can also be used to give a cosmic trigger for testing and calibration of the ALICE detector using cosmic rays. The intensity of the charged penetrating component of cosmic rays (mainly muons) crossing a horizontal area is $1.3 \times 10^2 \text{ m}^{-2} \text{ s}^{-1}$ at sea level. This gives a particle rate crossing the ScB of the order of $4 \times 10^3 \text{ s}^{-1}$. Taking into account that testing runs can be as long as two months ($5 \times 10^6 \text{ s}$), we can expect up to 2×10^{10} cosmic ray events per run, which is quite sufficient for the setup testing and calibration.

The cosmic trigger would work asynchronously. The logic of the trigger should be based on 'hit' signals (H-signals) from 24 supermodules of the ScB.

A H-signal from one of the 12 supermodules in the upper hemisphere of the barrel can be used as the master signal to open a 40 ns time gate. In the most simple case the master signal should be in coincidence with a H-signal from one of the 12 supermodules in the lower hemisphere during the gating time. The trigger rate is $\sim 4 \times 10^3 \text{ s}^{-1}$ in this case, while the noise rate will be negligible small ($\sim 2 \text{ events/s}$ for a PMT noise of 10^4 Hz per channel).

For cosmic tests of different detectors one can foresee also other requirements of the signal coincidence from combinations of the barrel supermodules. The neural net electronics would be quite useful in this case.

8 Cost estimation

In the following table detail cost estimations of production and assembly of the scintillator barrel are presented. Today's price levels on materials and machining in Russia and in the world are taken into account.

Scintillator tiles	6.3 kCHF
material	polystyrene
dopants	1.5%PT+0.01%POPOP
weight	834 kg(6.3CHF/kg)
number	3360
square	180 m^2
Production of plates	25 kCHF
TOTAL	31.3 kCHF (174CHF/ m^2 ,37CHF/kg)
Fibers	35 kCHF
type	Y11(KURARAY)
length	50 km (0.7CHF/m)
number	13440
Evaporating mirror	7 kCHF
TOTAL	42 kCHF(0.84CHF/piece)
Support of tiles	9 kCHF
square	90 m^2
material	honeycomb
TOTAL	9 kCHF(100CHF/ m^2)
Assembly of tiles	23.5 kCHF
Assembly of megatiles	14 kCHF
TOTAL (detector)	119.8 kCHF
New multianode PMT (HAMAMATSU)	480 kCHF
Multianode PMT (H5828, HAMAMATSU)	672 kCHF
Electronics	67.2 kCHF(20CHF/channel)
TOTAL (read out)	547.2 kCHF
TOTAL	667 kCHF

9 Future R&D program

The following R&D investigations are very important for improvement of the ScB characteristics:

- optimization of the light collection with scintillator tiles by WLS fibers;
- study of multianode photomultipliers, pixel hybrid photomultipliers, avalanche photodiodes and other types of photodetectors;
- production and test of the full scale prototype of the ScB supermodule;
- design, production and test of the trigger electronics prototype.

In conclusion we would like to thank K.Kuroda for useful discussions and fruitful cooperation.

References

- [1] CERN/LHCC/95-71, ALICE Technical Proposal, 15 December 1995.
- [2] S.A.Sadovsky, ALICE/95-30 Internal Note/Phys, October 1995.
- [3] V.I. Kryshkin and A.I. Ronzhin. Nucl.Instrum. Methods A247 (1986) 583.
- [4] M.G. Albrow et al., Nucl.Instrum. Methods A256 (1987) 23.
- [5] V. Agoritsas et al., CERN/DRDC 91-8, DRDC/P25.
V. Agoritsas et al., RD-17 Status Report, CERN/DRDC 93-47.
A.M. Gorin et al., Nucl.Instrum. Methods A344 (1994) 220. V. Agoritsas et al.,
Preprint LAPP LAPP-EXP-95.01.
- [6] K. Kuroda. private communication.
- [7] 80170NX Electrically Trainable Analog Neural Network Data Booklet. Intel Corp. 22550 Mission College Boulevard, Santa Clara, CA 95052-8125, USA
- [8] iNNTS Neural Network Training System Users's Guide. Intel Corp. (1992)
- [9] P. Masa et al., Proceedings 'Fourth Intern.Conf. on Microelectronics for Neural Networks and Fuzzy Systems', Turin 1994.